

Time-scale analysis of quadrature Doppler ultrasound signals

N.Aydin and H.S.Markus

Abstract: Most Doppler ultrasound systems employ quadrature demodulation techniques at the detection stage. The information concerning flow direction, encoded in the phase relationship between in-phase and quadrature-phase channels, is not obvious at this stage. The complex fast Fourier transform can be used to obtain directional information in the frequency domain, as well as time-frequency analysis of Doppler signals. However, it has an inherent time-frequency resolution limitation. The wavelet transform allows the time-frequency resolution compromise to be optimised. Mapping directional information in the scale domain is also desirable. A method is described, based on the utilisation of complex wavelets and negative scales. It eliminates the intermediate processing stages for obtaining directional Doppler signals for time-scale analysis.

1 Introduction

Most Doppler ultrasound systems employ quadrature demodulation techniques at the detection stage of the system [1]. The incoming radio frequency signal from an ultrasonic transducer is multiplied by a 90° phase-shifted version of the transmitted signal as well as the transmitted signal. After filtering out the high-frequency components, in-phase and quadrature-phase components of the audio Doppler signal are obtained. The information concerning flow direction, which is encoded in the phase relationship between in-phase and quadrature-phase channels, is not obvious at this stage. To extract directional information, further processing is necessary [2]. The complex fast Fourier transform (FFT) applied to quadrature Doppler signals provides the directional information in the frequency domain [3]. The FFT results are displayed as a sonogram, which is basically a form of windowed Fourier transform (WFT) involving processing data frames of fixed duration. The signal is assumed stationary within this analysis frame. In practice however, most natural signals, including Doppler signals, are non-stationary.

An alternative approach to the time-frequency (TF) analysis of non-stationary signals is the wavelet transform (WT). It has been shown that the WT is well suited to the analysis of Doppler signals, especially those containing short-lived embolic signals [4]. Emboli are much larger particles than red blood cells within blood circulation. They cause a short duration transient increase in intensity, which is greatest across a narrow frequency range when they pass through the sample volume [5]. Under certain conditions, embolic signals appear to be markers of increased stroke risk and may be useful in patient management [6]. The WT has also been used successfully to analyse, model, and

compute turbulent flows [7]. The WT, which has been increasingly applied in many fields [8, 9] including biomedical engineering [10, 11] is a promising technique for the analysis of Doppler ultrasound signals. It allows the TF resolution compromise to be optimised for the TF analysis of a signal. The WT has not been as widely used for the analysis of the quadrature Doppler signals as it has been used in other fields. In this respect, some of the important issues related to analysis of quadrature Doppler signals using the WT are highlighted here. A method is also described for mapping directional Doppler flow information in the scale domain.

2 Theory

2.1 Wavelet transform and time-scale analysis

The WT analysis is a relatively recent mathematical development, with many powerful applications in the analysis of real-world signals and images. A complete WT process creates a two-dimensional time-scale (TS) representation of a one-dimensional signal; typically the horizontal axis represents time and the vertical axis corresponds to the wavelet scale. The third dimension (colour in a two-dimensional display) is the amplitude of the WT coefficients. This representation allows the exact localisation of any abrupt change, or an exact time and duration to be attributed to a short signal, which may not be evidenced by conventional signal processing techniques. The continuous WT is performed by projecting a signal $s(t)$ onto a family of zero-mean functions (the wavelets) derived from an elementary function $\psi(t)$ (the mother wavelet) by translations and dilations, and given by

$$W_s(a, b) = |a|^{-1/2} \int_{-\infty}^{+\infty} s(t) \psi^* \left(\frac{t-b}{a} \right) dt \quad (1)$$

where $*$ denotes the complex conjugate and $\psi^*(t)$ is the analysing wavelet. The variable a ($\neq 0$) controls the scale of the wavelet, such that taking $a > 1$ dilates the wavelet ψ and taking $a < 1$ compresses ψ . The variable b is the time translation and controls the position of the wavelet.

© IEE, 2001

IEE Proceedings online no. 20010106

DOI: 10.1049/ip-smt:20010106

Paper first received 24th May and in revised form 5th September 2000

The authors are with the Division of Clinical Neuroscience, St George's Hospital Medical School, Cranmer Terrace, London SW17 0RE, UK

The WT is characterised by the following properties:

- (i) it is a linear transformation
- (ii) it is covariant under translations

$$s(t) \rightarrow s(t - u), W_s(a, b) \rightarrow W_s(a, b - u) \quad (2)$$

- (iii) it is covariant under dilations

$$s(t) \rightarrow s(kt), W_s(a, b) \rightarrow k^{-1/2} W_s(ka, kb) \quad (3)$$

Unlike the WFT, when the scale factor a is changed, the duration and bandwidth of the wavelet are both changed but its shape remains the same, as seen in Fig. 1b. The WT uses short windows at high frequencies and long windows at low frequencies. The bandwidth B is proportional to the frequency ω .

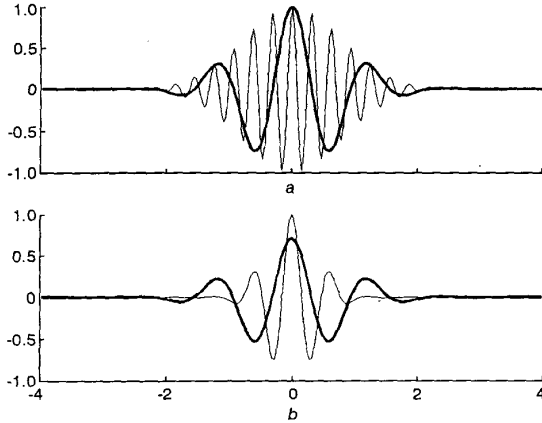


Fig. 1 Real parts of wavelet and Fourier bases
a Real parts of low-frequency and high-frequency Fourier bases
— low-frequency
— high-frequency
b Real parts of high-scale and low-scale wavelet bases
— high-scale
— low-scale

A signal $s(t)$ can be restored from its WT $W_s(a, b)$ using the formula:

$$s(t) = \frac{1}{C_\psi} \int_{-\infty}^{+\infty} \int_{-\infty}^{+\infty} W_s(a, b) \psi\left(\frac{t-b}{a}\right) \frac{dadb}{a^2} \quad (4)$$

providing that the Fourier transform of the wavelet $\psi(t)$, denoted $\Psi(\omega)$, satisfies the following admissibility condition:

$$C_\psi = \int_{-\infty}^{+\infty} \frac{|\Psi(\omega)|^2}{\omega} d\omega < \infty \quad (5)$$

This shows that $\psi(t)$ has to oscillate and decay.

2.2 Complex wavelets

If a signal is real, its FT coefficients are symmetric about the origin (Hermitian symmetry) and no information is lost by considering only their positive frequency parts. However, in many applications it is useful to work with complex signals, as this allows the representation of a modulated band-limited signal as its base-band equivalent. In this case, the FT coefficients are no longer symmetric, and both the positive and negative frequency parts of the spectrum should be considered independently. Likewise, it is convenient to work with the analytic wavelets rather than real ones in this case. The real wavelets are often used to detect sharp signal transitions, whereas the complex wavelet, which can separate amplitude and phase components, can be used to measure the time evolution of frequency transients [12].

Audio signals obtained from a Doppler ultrasound system employing the quadrature demodulation technique can be considered as complex quadrature signals [1]. A signal $s(t)$ is said to be analytic if its FT, $S(\omega)$, is zero for negative frequencies. Mathematically, complex quadrature Doppler signals with only positive frequency components are analytic signals. In the context of the quadrature Doppler signals, an analytic signal is a subset of the complex quadrature signals, in which both positive and negative frequency components have a physical meaning. The complex FT of such a signal reveals directional information in the frequency domain. By using this information, signals with a positive frequency spectrum representing forward flow can be extended analytically to the upper half-complex time plane. Similarly, signals with a negative frequency spectrum representing reverse flow can be extended analytically to the lower half-complex time plane [13]. Their respective FTs can be given as

$$S_f(\omega) = \begin{cases} 2S(\omega) & \text{if } \omega \geq 0 \\ 0 & \text{if } \omega < 0 \end{cases} \quad (6a)$$

$$S_r(\omega) = \begin{cases} 0 & \text{if } \omega \geq 0 \\ 2S(\omega) & \text{if } \omega < 0 \end{cases} \quad (6b)$$

The existence and usefulness of a negative scale for the WT analogous to that of a negative frequency spectrum in the FT for the complex quadrature signals bear scrutiny. The latter is ensured by use of the complex exponential. A comparable property for the WT can be attained by the use of complex wavelets. The WT for processing quadrature Doppler signals can be implemented in such a way that wavelet coefficients resulting from the forward flow components are obtained when the scale is positive, and the wavelet coefficients resulting from the reverse flow components are obtained when the scale is negative. If the FT of a mother wavelet $\psi(t)$ is defined as $\Psi(\omega) = \Psi^+(\omega) + \Psi^-(\omega)$ (sum of its positive and negative frequency components), in addition to the required standard properties, such a wavelet must also satisfy the following property:

$$\Psi(\omega) = \begin{cases} \Psi^+(\omega) & \text{if } a > 0 \\ \Psi^-(\omega) & \text{if } a < 0 \end{cases} \quad (7)$$

This is attained by the sine-cosine formulation, which naturally exists in some common wavelets such as Morlet and Cauchy wavelets [14].

2.2.1 Morlet wavelet: This is a locally periodic wave-train, obtained by localising a complex sine wave with a Gaussian envelope, as given by

$$\psi(t) = e^{i\omega_0 t} e^{-t^2/2} \quad (8)$$

where ω_0 is non-dimensional frequency and usually assumed to be 5 to 6 to satisfy the admissibility condition. Since the directional coefficients are directly defined by the scale parameter a , ignoring the translation parameter b , the scale-dependent Morlet wavelet is

$$\psi(t/a) = e^{i\omega_0 t/a} e^{-t^2/2a^2} \quad (9)$$

The FT of the scale-dependent Morlet wavelet is given by

$$\Psi(\omega) = \begin{cases} |a| \sqrt{2\pi} e^{-\frac{(\omega_0 - a\omega)^2}{2}} H(\omega), & a > 0 \\ |a| \sqrt{2\pi} e^{-\frac{(\omega_0 + a\omega)^2}{2}} H(-\omega), & a < 0 \end{cases} \quad (10)$$

where H is the Heaviside step function, defined as

$$H(\omega) = \begin{cases} 1, & \omega > 0 \\ 0, & \omega < 0 \end{cases} \quad (11)$$

From eqn. 10, we can observe that a frequency spectrum of an upper analytic wavelet is obtained for $a > 0$ and a frequency spectrum of a lower analytic wavelet is obtained for $a < 0$.

2.2.2 Cauchy wavelet: This is also a complex exponential function, given by

$$\psi(t) = \frac{\Gamma(m+1)}{2\pi(1-it)^{(m+1)}} \quad (12)$$

where $m (> 0)$ is the order of the wavelet, and the gamma function is defined by

$$\Gamma(m) = \int_0^{+\infty} t^{m-1} e^{-t} dt \quad (13)$$

Again ignoring the translation parameter b , the scale-dependent Cauchy wavelet is given by

$$\psi(t/a) = \frac{\Gamma(m+1)}{2\pi} \left(1 - i\frac{t}{a}\right)^{-(m+1)} \quad (14)$$

Taking the FT of eqn. 14 reveals the directionality property of this wavelet:

$$\Psi(\omega) = \begin{cases} a^{m+1} \omega^m e^{-a\omega} H(\omega), & a > 0 \\ a^{m+1} (-\omega)^m e^{a\omega} H(-\omega), & a < 0 \end{cases} \quad (15)$$

The Morlet and Cauchy wavelets with corresponding frequency spectra (only upper analytic wavelets) are shown in Fig. 2.

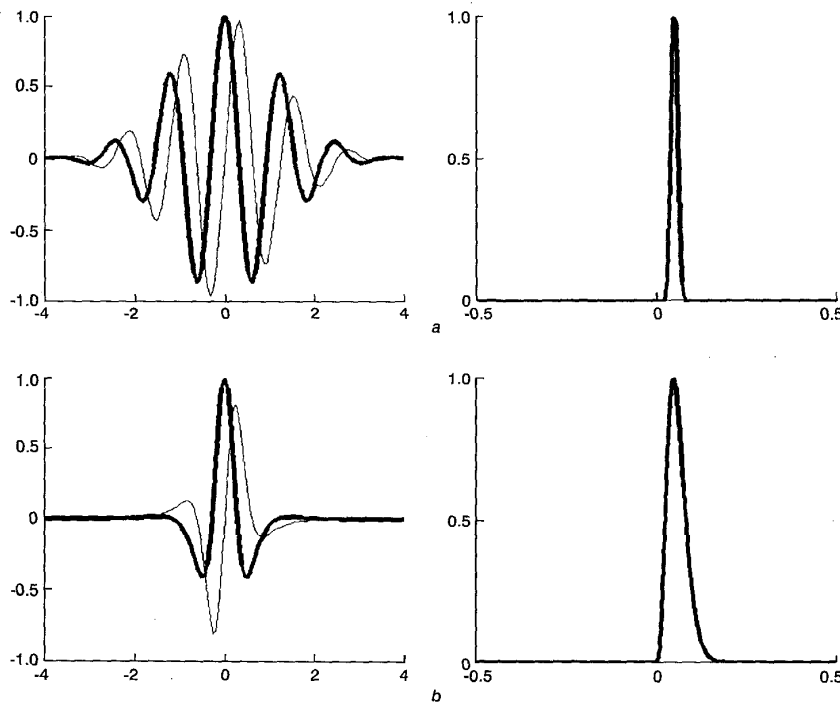


Fig. 2 Real and imaginary components of two complex wavelets (left) and respective frequency spectra (right)
 — real
 - - - imaginary
 a Morlet
 b Cauchy wavelet ($n = 4$)

3 Method

To see how negative scales have been utilised for obtaining directional wavelet coefficients, let us evaluate the WT equation for the Morlet wavelet. In this case, the specific form of the WT of a signal $s(t)$ is given by

$$W_s(a, b) = |a|^{-1/2} \int_{-\infty}^{+\infty} s(t) e^{\frac{i\omega_0(t-b)}{a}} e^{-\frac{(t-b)^2}{2a^2}} dt \quad (16)$$

This is simply a convolution of the signal $s(t)$ with the Morlet wavelet. A complete set of directional wavelet coefficients can be mapped over the scales from $a = -J$ to $a = J$, excluding $a = 0$, by evaluating eqn. 16. Plots of the

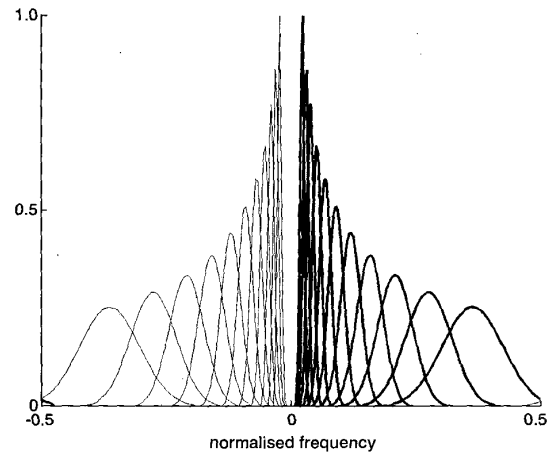


Fig. 3 Plot of the complex Morlet wavelet spectra for 22 different scales ($-11 < a < 11$)
 — upper analytic wavelets
 - - - lower analytic wavelets

frequency spectra for the Morlet wavelet for a range of negative and positive scales are shown in Fig. 3. To demonstrate this mathematically, let the translation parameter $b = 0$ for simplicity. Then

$$W_s(a, 0) = |a|^{-1/2} \int_{-\infty}^{+\infty} s(t) e^{i\omega_0 t/a} e^{-0.5t^2/a^2} dt \quad (17)$$

For $a = 1$ and $a = -1$, the WT of the signal $s(t)$ is given, respectively, by

$$W_s(1, 0) = \int_{-\infty}^{+\infty} s(t) e^{i\omega_0 t} e^{-0.5t^2} dt \quad (18a)$$

$$W_s(-1, 0) = \int_{-\infty}^{+\infty} s(t) e^{-i\omega_0 t} e^{-0.5t^2} dt \quad (18b)$$

The wavelets used in eqns. 18a and b can be properly renamed as the upper analytic wavelet and the lower analytic wavelet, respectively. It transpires that the upper analytic wavelet and the lower analytic wavelet are closely related to their counterpart analytic Fourier components. Since the WT is equivalent to the convolution of the wavelet function and the signal under investigation, it can be easily implemented using the fast convolution; this corresponds to taking Fourier transforms of the wavelet function and the signal independently and multiplying them in the frequency domain [15]. Taking the FT of eqn. 18a and b yields, respectively

$$F\{W_s(1, 0)\} = CS(\omega) e^{-\frac{(\omega_0 - \omega)^2}{2}} H(\omega) \quad (19a)$$

$$F\{W_s(-1, 0)\} = CS(\omega) e^{-\frac{(\omega_0 + \omega)^2}{2}} H(-\omega) \quad (19b)$$

where $S(\omega)$ is the FT of the signal $s(t)$, and C is a constant. Inverse Fourier transforms of eqns. 19a and b yield com-

plex wavelet coefficients formed by only the forward and the reverse flow components, respectively.

In the case of the Cauchy wavelet with $m = 4$, assuming $b = 0$, for $a = 1$ and $a = -1$, directional wavelet coefficients in the frequency domain are

$$F\{W_s(1, 0)\} = CS(\omega) \omega^4 e^{-\omega} H(\omega) \quad (20a)$$

$$F\{W_s(-1, 0)\} = CS(\omega) (-\omega^4) e^{\omega} H(-\omega) \quad (20b)$$

where $S(\omega)$ is the FT of the signal $s(t)$ and C is a constant.

3.1 Simulation and applications

A simple simulated signal, comprising both forward and reverse flow components, can be used to test the algorithm;

$$s(t) = e^{i2\pi f_f t} [u(t) - u(t - t_1)] + 0.5 e^{-i2\pi f_r t} [u(t - t_1) - u(t - t_2)] \quad (21)$$

where u is the unit step function, and f_f and f_r represent forward and reverse flow frequency components, respectively. The quadrature signal given in Fig. 4a consists of two complex signals representing constant forward ($F_s = 7150\text{Hz}$, $f_f = 1500\text{Hz}$) and reverse flows ($F_s = 7150\text{Hz}$, $f_r = 250\text{Hz}$) signal components, length of 512. The forward flow signal stops and the reverse flow signal starts at time t_1 (35.8ms), as illustrated in Fig. 4b. The TF plot (modulus of the complex WFT), the TS plots (modulus of the complex WT) with the Morlet and Cauchy wavelets, and related phase plots (phase of the complex WFT and WT) are shown in Fig. 4. The complex WT algorithm maps directional information in the scale domain as the complex WFT does in the frequency domain. The phase plot of the complex WT is also more informative than the WFT. The transition point from one frequency to another is defined very clearly in Figs. 4f and h.

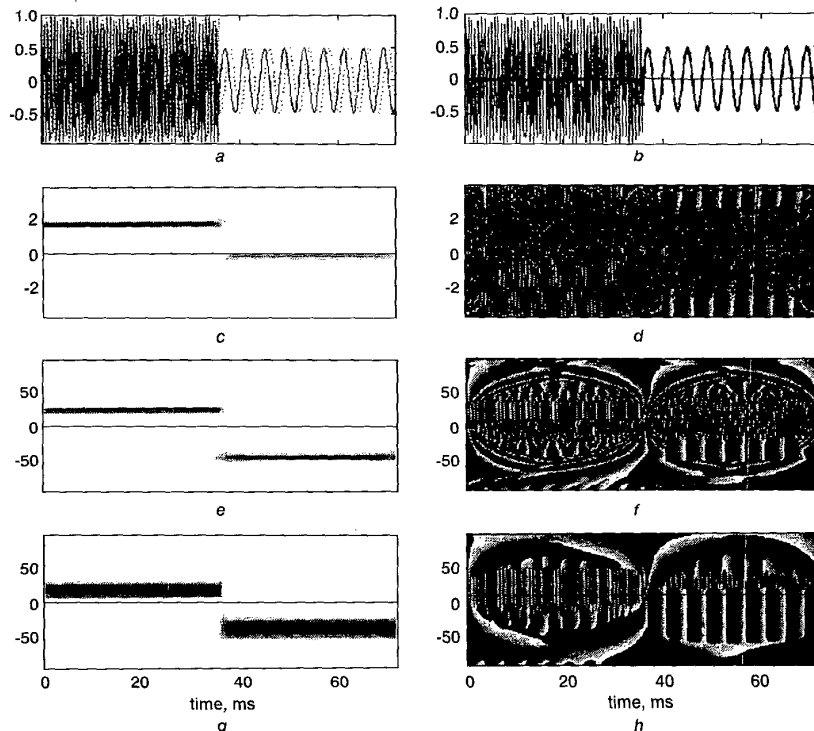


Fig. 4 Quadrature signal
a Simulated complex quadrature signal having two monotonic signals at each direction; b Corresponding directional signals; c TF; d Phase plots associated with c; e, g TS; f, h Phase plots associated with e, g

Although the relationship between the equivalent Fourier period and the wavelet scale can be derived analytically for a particular wavelet function [16, 17], the convention is to use TS representation for the WT. As an analogy to the Fourier energy spectrum, a wavelet energy spectrum can be obtained by integrating the TS representation of a signal over the time. Similarly, an instantaneous envelope of a signal can be obtained by integrating the TS representation of a signal over the scales (Fig. 5). A quadrature

embolic Doppler signal, which is recorded from a patient with symptomatic carotid stenosis by a transcranial Doppler system, and respective directional signals, its TF plot, TS plots using Morlet and Cauchy wavelets, and corresponding instantaneous envelopes and averaged Fourier and wavelet energy spectra are illustrated in Fig. 5.

Fig. 6 depicts a normal Doppler signal obtained from the common carotid artery of a healthy subject and corresponding TF plot, TS plots with Morlet and Cauchy

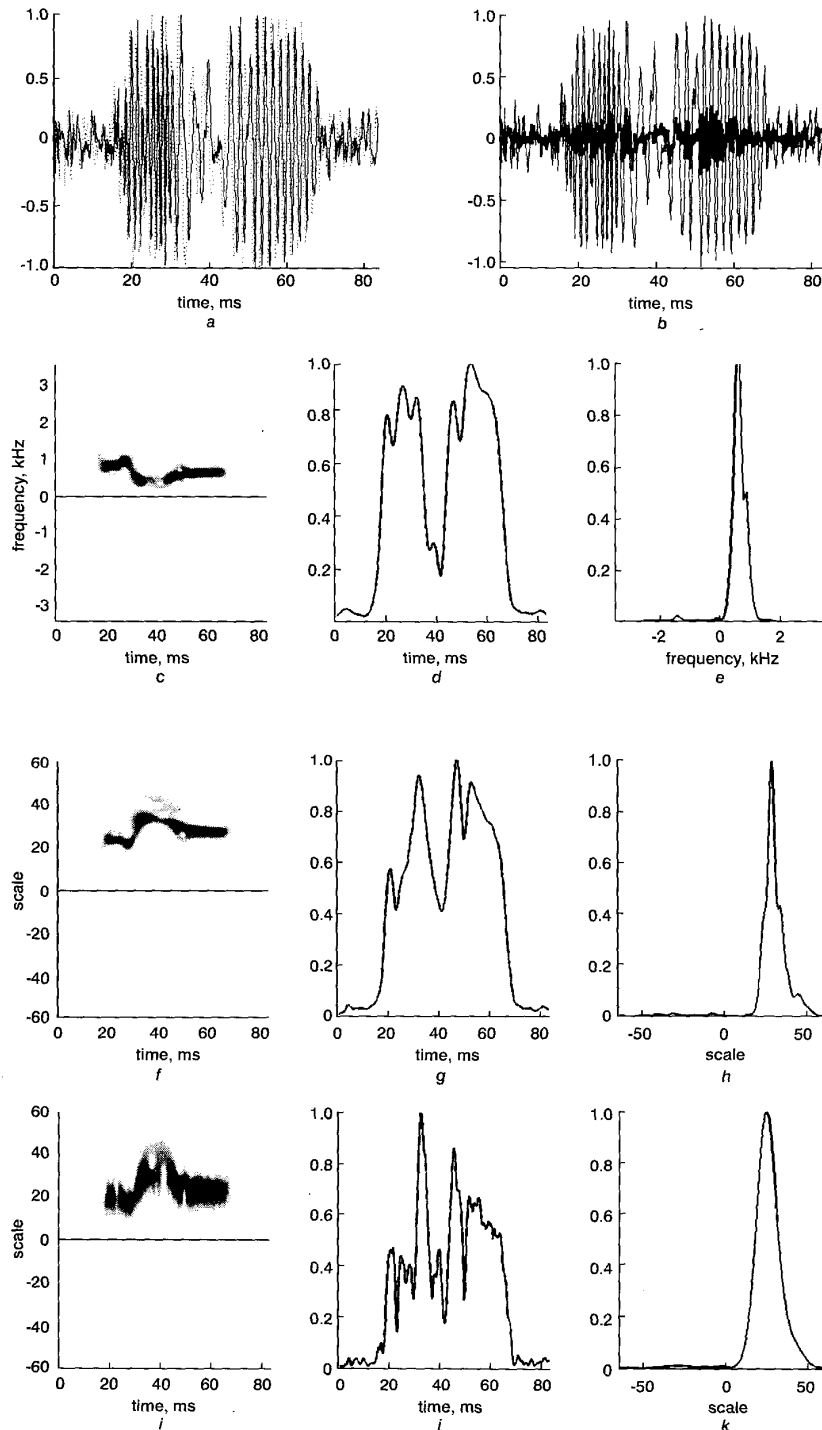


Fig. 5
a Embolic quadrature Doppler signal; *b* Corresponding directional signals; *c* TF plot and TS plots for *f* and *i*; *d, g, j* Associated instantaneous envelopes; *e, h, k* Averaged Fourier and wavelet energy spectra; *f* Morlet wavelet; *i* Cauchy wavelet

wavelets, respective instantaneous envelopes, and averaged Fourier and wavelet energy spectra. Figs. 7 and 8 show a directional low-intensity embolic signal corrupted by a bidirectional low-frequency artefact and respective 3-D TF and TS plots. The sampling frequency for all signals was 7150Hz. A 98.4% overlapped 64 points complex FFT with a Hanning window was used for the TF analysis. For the TS analysis, 64 scale complex Morlet and Cauchy wavelets were used.

4 Results and conclusions

Unlike the WFT, the WT provides good frequency resolution for low-frequency signals and good time resolution for high-frequency signals, and hence an optimised TS localisation as evidenced in the TF and the TS plots in Figs. 4–8. This optimisation allows the WT to simultaneously capture an abrupt change and a slowly changing trend in a signal. The phase of the complex WT is also

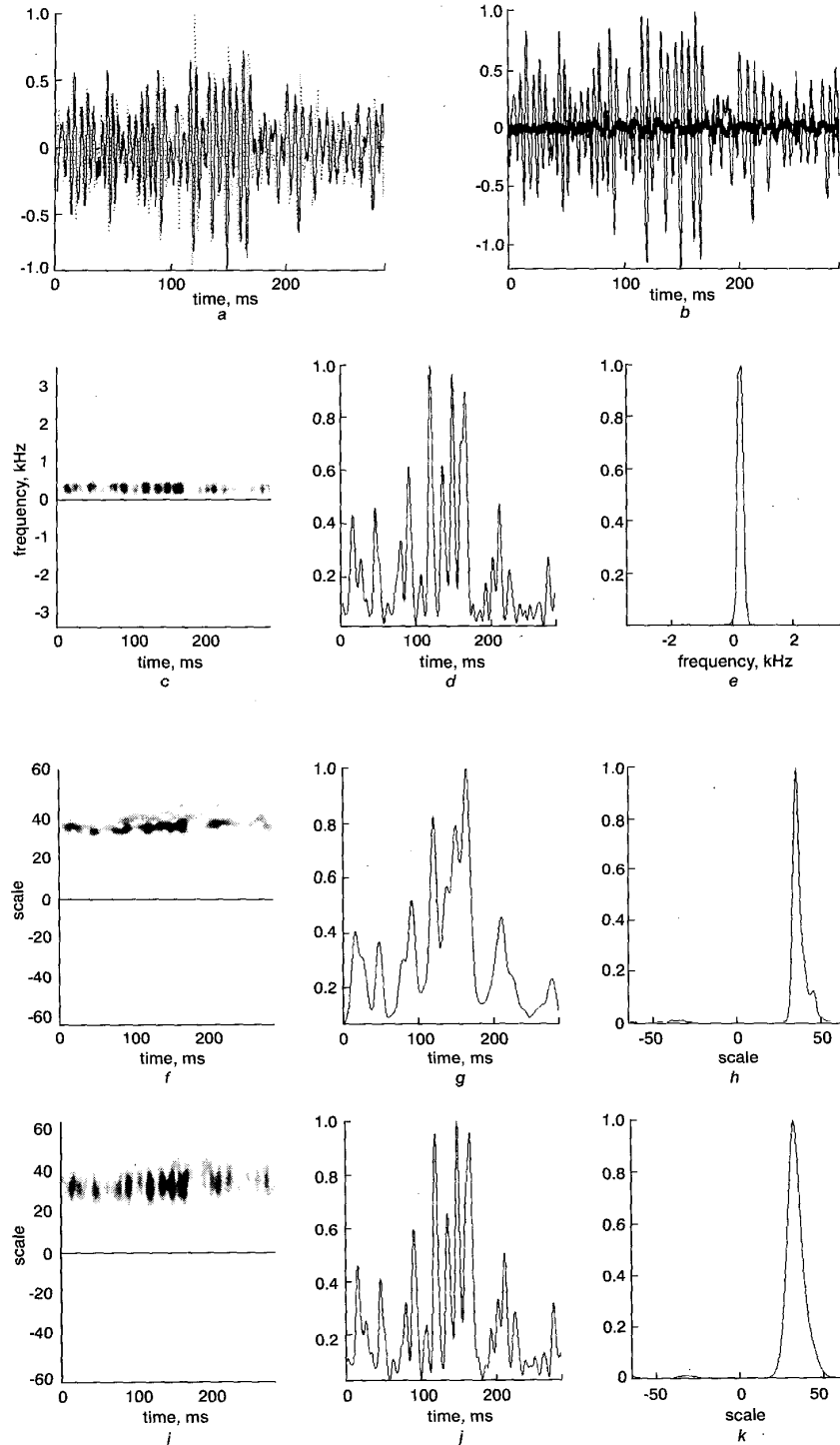


Fig. 6
a Normal quadrature Doppler signal obtained from the common carotid artery; *b* Corresponding directional signals; *c* TF plot and TS plots for *f* and *i*; *d, g, j* Associated instantaneous envelopes; *e, h, k* Averaged Fourier and wavelet energy spectra; *f* Morlet wavelet; *i* Cauchy wavelet

useful in detection of singularities in a signal as shown in Figs. 4*f* and *h* as the phase lines converge towards the point where the singularity exists. In the case of the WFT, three important parameters must be defined prior to analysis; window size, window type, and overlap ratio. The TF result with the WFT is a function of the analysis window size and the non-stationary signal duration. A short window introduces spread in frequency space and a long window introduces spread in time space, leading to a blurred TF representation of the signal being analysed [18]. The assumption is made that the signal to be analysed is stationary within the analysis window. If the properties of the signal of interest do not change within the analysis window, the WFT analysis with an appropriate window size is likely to yield the desired TF representation of the signal. However, the presence of a signal of interest shorter than analysis window size invalidates this assumption. In practice, statistical properties of a non-stationary signal cannot be known prior to the analysis. Hence the success of the WFT analysis is bounded by the right choice of window size and function. In the WT case, this limitation is eliminated by projecting the signal of interest on multiple scales (window sizes). The TS representations shown in Figs. 5*f* and *i* for the signal in Fig. 5*a* are comparable to the TF representation of the same signal with the 64-point WFT (Fig. 5*e*), in which the FFT parameters were optimised for this particular signal. The TS representation of the Doppler signal shown in Fig. 6*f* appears to be better as the frequency contents of the signal are better described, and the description of the time evolution is comparable to the TF representation of the Doppler signal given in Fig. 6*c*.

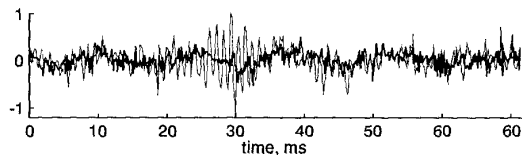


Fig. 7 Forward and reverse signals of a low intensity short embolic Doppler signal corrupted by a low frequency bi-directional artefact

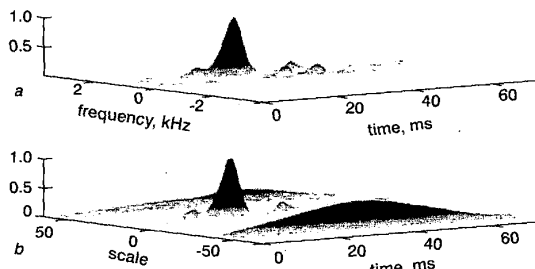


Fig. 8 Three-dimensional TF and TS plots corresponding to Fig. 7

Bidirectional low-frequency signal components (Fig. 7), resulting from a low-frequency artefact, are almost lost in the 3-D TF plot due to poor frequency resolution (Fig. 8*a*). On the other hand, they are clearly visible in the 3-D TS plot (Fig. 8*b*) with a comparable description of the short embolic signal as this is important to discriminate low-intensity embolic signals from large artefacts. However, rather like the effects of the window size on the WFT results, the WT results are affected by the type of wavelet chosen for analysis. This is clearly shown in the TS plots with two different wavelets presented in Figs. 4–6. The Morlet wavelet appears to give better frequency resolution, whereas the Cauchy wavelet has better temporal resolution

in the examples given above. The choice of wavelet is mainly dictated by the goals of the analysis. If one knows the characteristics of the signal or pattern being sought, the wavelet should be chosen to have a similar pattern.

The continuous WT algorithm is computationally more intensive when compared to the WFT with maximum overlap. A WT algorithm implemented using a discrete equivalent of eqn. 1 with 32 scales requires approximately 40 times more computation than a 64-point WFT for processing a signal with 1024 data points. However, the use of fast algorithms allows the WT to be computed more efficiently. As an example, the WT algorithm based on the fast convolution requires only three times more computational power than the WFT for the same signal. Computational efficiency can also be improved by approximating the WT at a required accuracy [19].

We have described a method to obtain directional wavelet coefficients from quadrature Doppler signals. Although there is much excellent work on wavelets, almost all of it concentrates on positive scales. Negative scales and their use have not been treated properly in a physical context. The use of complex wavelets allows negative and positive scales to be utilised in order to map directional wavelet coefficients. From the results, we can conclude that the described complex WT yields the wavelet coefficients resulting from the signal components with only a positive frequency spectrum for the positive scales. On the other hand, negative scales will produce the wavelet coefficients resulting from the signal components with only a negative frequency spectrum. By the proposed method, intermediate processing stages for obtaining directional Doppler signals for wavelet analysis have been eliminated. This method also eliminates the computational errors introduced by the FIR Hilbert transform and associated delay filters (which is the standard technique for obtaining directional time domain signals from quadrature Doppler signals), and reduces the computational requirements for wavelet analysis of complex quadrature Doppler signals. Furthermore, directional time domain signals can be reconstructed by simply evaluating reconstruction formulas. If the inverse WT is evaluated over the positive scales, the forward signal and associated Hilbert-transformed forward signal are obtained. If the inverse WT is evaluated over the negative scales, the reverse signal and associated Hilbert-transformed reverse signal are obtained.

Real-valued wavelets can also be modified to obtain directional wavelet coefficients. In this case, instead of using one mother wavelet, two wavelets should be used, constructed from the original real wavelet and its Hilbert transform. It is hoped that, with an understanding of the WT in a physical context, it will find increasing usage in the analysis and study of various quadrature signals, such as those arising in Doppler ultrasound. The results may also be extended to the discrete WT and associated fast implementations.

5 Acknowledgment

This work was supported by a British Heart Foundation project grant (PG99064).

6 References

- EVANS, D.H., McDICKEN, W.N., SKIDMORE, R., and WOODCOCK, J.P.: 'Doppler ultrasound: physics, instrumentation and clinical applications' (John Wiley & Sons Ltd, Chichester, 1989)
- AYDIN, N., FAN, L., and EVANS, D.H.: 'Quadrature-to-directional format conversion of Doppler signals using digital methods', *Physiol. Meas.*, 1994, **15**, pp. 181–199

- 3 AYDIN, N., and EVANS, D.H.: 'Implementation of directional Doppler techniques using a digital signal processor', *Med. Biol. Eng. Comput.*, 1994, **32**, pp. S157-S164
- 4 AYDIN, N., PADAYACHEE, S., and MARKUS, H.S.: 'The use of the wavelet transform to describe embolic signals', *Ultrasound Med. Biol.*, 1999, **25**, pp. 953-958
- 5 MARKUS, H.S., and TEGELER, C.: 'Experimental aspects of high-intensity transient signals in detection of emboli', *J. Clin. Ultrasound*, 1995, **23**, pp. 81-87
- 6 MARKUS, H.S., and HARRISON, M.J.: 'Microembolic signal detection using ultrasound', *Stroke*, 1995, **26**, pp. 1517-1519
- 7 FARGE, M., KEVLAHAN, N., PERRIER, V., and GOIRAND, E.: 'Wavelets and turbulence', *Proc. IEEE*, 1996, **84**, pp. 639-669
- 8 DAUBECHIES, I.: 'Where do wavelets come from? - a personal point of view', *Proc. IEEE*, 1996, **84**, pp. 510-513
- 9 SWELDENS, W.: 'Wavelets: what next', *Proc. IEEE*, 1996, **84**, pp. 680-685
- 10 AKAY, M.: 'Wavelets in biomedical engineering', *Ann. Biomed. Eng.*, 1995, **23**, pp. 531-542
- 11 UNSER, M., and ALDROUBI, A.: 'A review of wavelets in biomedical applications', *Proc. IEEE*, 1996, **84**, pp. 626-638
- 12 MALLAT, S.: 'A wavelet tour of signal processing' (Academic Press, San Diego, USA, 1998)
- 13 KAISER, G.: 'A friendly guide to wavelets' (Birkhäuser, Boston, USA, 1994)
- 14 DAUBECHIES, I.: 'The wavelet transform time-frequency localization and signal analysis', *IEEE Trans. Inf. Theory*, 1990, **36**, pp. 961-1004
- 15 HOLSCHEIDER, M.: 'Wavelets: an analysis tool' (Clarendon Press, Oxford, UK, 1995)
- 16 MEYERS, S.D., KELLY, B.G., and O'BRIEN, J.J.: 'An introduction to wavelet analysis in oceanography and meteorology: with applications to the dispersion of Yanai waves', *Mon. Weather Rev.*, 1993, **121**, pp. 2858-2866
- 17 TORRENCE, C., and COMPO, G.P.: 'A practical guide to wavelet analysis', *Bull. Am. Meteorol. Soc.*, 1998, **79**, pp. 61-78
- 18 AYDIN, N., and MARKUS, H.S.: 'Optimisation of processing parameters for the analysis and detection of embolic signals', *Eur. J. Ultrasound*, 2000, **12**, pp. 69-78
- 19 UNSER, M., ALDROUBI, A., and SCHIFF, S.J.: 'Fast implementation of the continuous wavelet transform with integer scales', *IEEE Trans. Signal Process.*, 1994, **42**, pp. 3519-3523